

Configuration of the Optic Chiasm in Humans with Albinism as Revealed by Magnetic Resonance Imaging

Bernd Schmitz,¹ Torsten Schaefer,¹ Christoph M. Krick,¹ Wolfgang Reith,¹ Martin Backens,¹ and Barbara Käsmann-Kellner²

PURPOSE. To determine whether the size and configuration of the optic chiasm in humans with albinism is different from that in normal control subjects.

METHODS. Seventeen patients and 15 control subjects underwent magnetic resonance imaging of the entire head. Images were reformatted to the chiasm region and analyzed with observer-independent morphometry and measurements by a blinded observer.

RESULTS. The albino group showed significantly smaller chiasmatic widths, smaller optic nerves and tracts, and wider angles between nerves and tracts. Statistical morphometry showed a different configuration of the optic chiasm.

CONCLUSIONS. Size and configuration of the optic chiasm in humans with albinism are distinctly different from those in normal control subjects and reflect the atypical crossing of optic fibers. (*Invest Ophthalmol Vis Sci.* 2003;44:16-21) DOI: 10.1167/iovs.02-0156

Axons of retinal ganglion cells form crossed and uncrossed projections at the optic chiasm in a way that information from the temporal hemifield of each eye is transmitted to the contralateral cerebral hemisphere. This optic hemidecussation is a principal element in binocular vision in humans¹ and provides an anatomic basis for the ocular dominance columns in the visual cortex.

The long-standing evidence of congenital misrouting of optic fibers in albinism was originally reported in anatomic² and electrophysiological³ studies. Most fibers from each eye cross to the contralateral lateral geniculate nucleus. The reasons for this are probably disturbances in the developmental timing in the albino retina. One factor that causes growing axons in the chiasm region to cross or remain ipsilateral is the time when the axons reach the chiasm region.⁴ The peak in the production of uncrossed cells in the mouse is 2 days ahead of the peak production of crossed cells. Furthermore, Ilia and Jeffrey⁵ showed that dopa, which is a precursor in melanin synthesis, is a major regulator of retinal cell differentiation and spatial organization and that it influences the capacity of cells to exit the cell cycle. In a recent review, Jeffery⁶ concludes from these studies that a delay in ganglion cell production in albinism leads to the abnormal projection pattern through the chiasm.

In rodents and carnivores, crossed and uncrossed fibers are mixed throughout the whole chiasm.⁷⁻⁸ However, there is strong evidence that uncrossed fibers remain confined laterally

in the human and nonhuman primate optic nerve and chiasm.^{9,10} Anatomic studies using anterograde¹¹ or retrograde¹² tracers have shown that the lateral group of optic fibers enters the ipsilateral optic tract without reaching the midline.

Summarizing the facts of predominant crossing of retinogeniculate fibers in humans with albinism and the confinement of uncrossed fibers to the lateral aspects of the chiasm, it is reasonable to assume that the lateral aspects of the chiasm in albinos should be less prominent macroscopically.

A study of magnetic resonance imaging (MRI) of the optic chiasm in humans with albinism,¹³ with 10 subjects and no control subjects included, failed to show configurational abnormalities, and the authors concluded that these abnormalities are probably too subtle to be detected by the resolution of MRI.

To reveal the assumed differences in chiasm architecture, we compared patients with albinism with normally pigmented control subjects in a larger sample with high-resolution MRI, by using classic measurements of the optic nerves, tracts, and optic chiasm on specially reformatted planes and by observer-independent statistical measurements.

METHODS

Subjects

Seventeen patients with oculocutaneous albinism (OCA; mean age, 31.0 ± 2.2 years, 11 women) underwent a standardized morphologic evaluation^{14,15} including assessment of visual function and binocular interaction, examination for nystagmus, evaluation of refractive errors, transillumination of the iris, optic disc size, examination of the retina, and determination of hypopigmentation of the retinal pigment epithelium (all parameters morphologically graded). Binocularity was evaluated as the measurement of the angle of strabismus for far and near distance. In patients with small angles of strabismus or apparently no strabismus, binocular interaction was tested by the following tools in the order listed: Bagolini glasses, stereo fly, Lang II test, and Titmus rings. Pigmentation of the iris tissue and the retinal pigment epithelium and the size of the optic nerves were photodocumented with a standardized method. Iris transillumination was accomplished by a punctiform confocal transpupillary slit lamp light followed by the evaluation of the ratio of transilluminable tissue area to tissue that was not transilluminable (reflected red fundus light). Optic nerve head (ONH) size was evaluated by using the emerging vessels as a means for judging and comparing the size and the plane on which the ONH was positioned: flat in patients without tilted optic disc syndrome and nasally elevated in patients with the syndrome. Refractive errors were taken into account when judging the ONH size. All patients were seen by the primary ophthalmologic examiner (BKK). In 13 patients, an independent observer also performed the morphologic grading by examining the patient. All photodocumentation was seen by two independent observers. The documentation, however, provided sufficient grounds only for morphologic grading in 11 patients because the images were affected by the patients' having severe nystagmus.

Clinical history was obtained regarding photophobia, inability of the skin to tan, and family history of albinism. Tyrosinase gene-related OCA (OCA1) was diagnosed in eight patients by molecular genetic

From the Departments of ¹Neuroradiology and ²Ophthalmology, Saarland University Hospital, Homburg, Germany.

Submitted for publication February 11, 2002; revised July 31, 2002; accepted August 9, 2002.

Commercial relationships policy: N.

The publication costs of this article were defrayed in part by page charge payment. This article must therefore be marked "advertisement" in accordance with 18 U.S.C. §1734 solely to indicate this fact.

Corresponding author: Bernd Schmitz, Department of Neuroradiology, Saarland University Hospital, D-66424 Homburg, Germany; bernd.ludwig.schmitz@web.de.

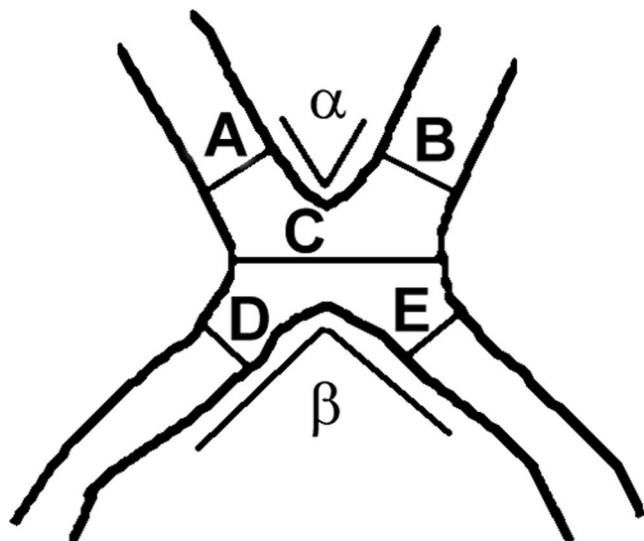


FIGURE 1. Schematic representation of the optic chiasm with positions and orientations of measured distances and angles. Diameters of the optic nerves were measured perpendicular to the long axis of the nerve, with the medial starting point 2 mm anterior to the frontal border of the optic chiasm (lines A and B). The width of the optic chiasm was measured at its smallest aspect (line C). Diameters of the optic tracts were measured 2 mm posterior to the occipital border of the optic chiasm, perpendicular to the tract (lines D and E). Angles between the optic nerves were measured by drawing lines along the middle of the optic nerves and taking the angle at the crossing point of these two lines. Angles between optic tracts were obtained in the same way. Angles were labeled α and β (lines in the figure are not in the positions measured in the middle of the tracts and nerves).

testing, P-gene (pink-eye dilution gene)-related OCA2 was diagnosed in four patients, and ocular albinism (OA)-1 in one. The other four patients are still under evaluation. Fifteen normal control subjects (mean age, 26.2 ± 0.7 years, 10 women) were clinically evaluated in the same way. All subjects gave written informed consent according to the Declaration of Helsinki.

Magnetic Resonance Imaging

All scans were made on a 1.0-Tesla scanner (Magnetom Expert Scanner; Siemens, Erlangen, Germany). First, a T_2 -weighted turbo spin-echo sequence (recovery time [TR] 4416 ms, echo time [TE] 99 ms, 5-mm slice thickness, 256×256 matrix) was obtained to exclude neurologic disease. Afterward, a T_1 -weighted three-dimensional magnetization-prepared rapid gradient-echo (MPRAGE) sequence¹⁶ (TR 15 ms, TE 7 ms, 1.0-mm slice thickness, 166 partitions, 256×256 matrix) was used to scan the entire head without gap, using a 1.0-mm^3 isotropic voxel size.

Morphologic Measurements

All images were transferred to a computer workstation (Omnipro; Marconi Medical Systems, Cleveland, OH) and a reformatted image (1.0-mm slice thickness) was obtained parallel to the optic nerves and tracts and through the optic chiasm. Measurements of the diameter of optic nerves and optic tracts, the width of the chiasm, and the angles between the optic nerves and tracts were performed by an experienced examiner as indicated in Figure 1. The images were masked as to the subjects' names and diagnoses and were presented by an independent person in a random order so that the observer performed the measurements in a blinded fashion. A second image perpendicular to the first was reconstructed through the middle of the optic chiasm to measure the height in the middle of the chiasm (not shown). Measurements of patients and control groups were compared on

computer by the nonparametric Mann-Whitney test (SPSS ver. 8.0; SPSS Science, Chicago, IL). The significance level was set at $P < 0.05$.

Observer-Independent Morphometry

In addition to the described subjective two-dimensional morphologic measurements, objective, observer-independent, voxel-based, three-dimensional morphometry was undertaken. To perform this analysis, we transferred all images to a second workstation running image-analysis software (Analyze ver. 7.5; Biomedical Imaging Resource; Mayo Foundation, Rochester, MN). A $50 \times 50 \times 30\text{-mm}$ subvolume of the whole brain scan was reconstructed, centered on the middle of the optic chiasm parallel to the optic nerves and tracts. This subvolume was interpolated to 0.3 mm^3 isotropic voxel size. Voxel intensities were scaled to the global mean of all images of patients and control subjects to account for intensity differences due to a different general scanner signal. Mean images were calculated for the patient and the control group. A three-dimensional Gaussian filter (full width at half maximum $2 \times 2 \times 2\text{ mm}^3$) was applied to the images using statistical parametric mapping (SPM99; Wellcome Department of Cognitive Neurology, University College London, Institute of Neurology, UK). Smoothing was critical, because, with the use of the central limit theorem, smoothing results in a more parametric distribution of the voxel values, allowing the use of standard parametric statistics.¹⁷ Because there is no widely accepted method to normalize head subvolumes, images of the chiasmal region were not normalized and individual differences were thereby preserved. To find voxels that show significant differences between the patients and control subjects, a two-sample *t*-test of the scaled intensities was calculated for each voxel by using SPM99. The theory of random Gaussian fields was used to assign significance to the resultant T-fields.^{18,19} The statistical T-map was thresholded at $P < 0.05$, corrected for multiple comparisons across the volume.

RESULTS

Results of the clinical examination of subjects with albinism are summarized in Table 1, with the grading system for pertinent findings in the examination described in Table 2. Examination of the normally pigmented control subjects did not reveal any ocular abnormality that pointed to a hypopigmentation disorder.

Reformatted images in single subjects (Figs. 2, 3), and the group mean images (Figs. 4, 5) parallel to the optic nerves and tracts showed differences in chiasm morphology. The chiasms of subjects with albinism looked more like an X, whereas chiasms in normal control subjects were shaped more like two back-to-back brackets. The most striking difference in the measurements was in the width of the chiasm, which differed significantly between patients ($10.3 \pm 0.8\text{ mm}$ [SD]) and control subjects ($12.9 \pm 0.8\text{ mm}$). Trends for correlations within the albino group between the level of visual dysfunction and size of the chiasm failed to reach statistical significance. The diameters of the optic nerves and tracts were significantly smaller in the albino group than in the normal control group, the angles between the optic nerves and tracts were larger in the albino group than in the normal control group. (Table 3). There were no significant differences in these parameters between the men and women in either group.

Observer-independent statistical morphometry confirmed the measured differences for the optic chiasm to be significant and in addition depicted more clearly that the difference was based on a different configuration in the lateral aspects of the optic chiasm which were more curved in the albino group (Fig. 6).

DISCUSSION

We compared the size and architecture of the optic chiasm between humans with albinism and normally pigmented con-

TABLE 1. Description of Patients with Albinism

Subject	Gender	Mean Visual	Skin	Skin Pigmentation	Hair	Hair Pigmentation	Iris Translucency	Fovea	ONH
GB	Female	0.1	1	1	3	2	3	3	3
FD	Female	0.25	3	2	5	2	3	4	4
CF	Male	0.2	1	1	1	1	4	3	4
AK	Female	0.07	1	1	3	2	4	4	4
MK	Male	0.15	2	1	8	2	3	4	4
WK	Male	0.2	5	3	9	2	3	3	3
SaK	Female	0.1	2	1	4	1	3	3	4
JK	Male	0.16	1	1	3	1	4	3	4
SuK	Female	0.35	2	1	5	1	2	3	4
KL	Female	0.1	1	1	1	1	4	3	3
KM	Male	0.08	1	1	1	1	4	4	4
HM	Male	0.01	1	1	1	1	4	4	4
CP	Female	0.2	1	1	5	2	3	3	2
AR	Female	0.14	1	1	3	1	3	3	3
BS	Female	0.1	1	1	3	1	4	3	4
PS	Female	0.1	1	1	1	1	4	4	3

The grades for each parameter are described in Table 2.

control subjects using high-resolution MRI and two different methods for measuring the differences. First, reformatted images parallel to the optic nerve and tract were measured by a blinded observer. The advantage in this approach is that quantitative results are obtained that can be compared with those in previous studies, and the disadvantage is that it is observer dependent. For normally pigmented subjects we measured a mean chiasmatic width of 12.9 ± 0.8 mm. This is in the range of previously published studies (10.3–18.3 mm),²⁰ but the mean was smaller than in these studies (14.0 mm,²⁰ 14.96 mm²¹). The same holds true for the mean diameters of the optic nerve and tract, which were also smaller in our study than in previous studies in normally pigmented subjects. Most probably, these differences are caused by the different methods used in our study. We used a 1.0-mm isotropic voxel size, whereas in both previous studies the investigators used 3.0-mm thick coronal slices. This larger slice thickness leads to partial volume effects that make the chiasm look wider, because it cannot be measured at its smallest aspect. This holds especially true for the optic nerves and tracts. The coronal slices measured by Parravano et al.²¹ and Wagner et al.²⁰ are oriented perpendicular to the optic chiasm, but this means that they are oblique to the optic nerves and tracts, which in turn makes the structures look wider than they really are. This is also obvious in the difference between height and width described previously (2.99 mm vs. 6.01 mm for the optic nerves) which is probably not real.

It was not the purpose of these studies to provide the true dimensions of the measured structures. These studies are valuable as references for clinical assessments, because the methods used are the standard and most appropriate methods for evaluating the chiasm region in clinical settings. In addition, the partial volume effects lead to a larger statistical range across which the optic chiasm width varies (10.5–18.5 mm²⁰ vs. 11.3–14.0 mm in our study). This smaller range may reflect the smaller sample size, but may also show the more exact method of measuring in our study. We measured axial planes, parallel to the optic nerves and tracts, clearly identifying the smallest part of the chiasm, and we used diameters perpendicular to the optic nerves and tracts, and so it is reasonable that our measurements show smaller means. However, we cannot exclude that our normally pigmented control subjects had smaller chiasms by chance, but our finding even smaller chiasms (10.3 \pm 0.8 mm) in our subjects with albinism makes the difference even more distinct.

TABLE 2. Grade Scales for Each Parameter

Skin	
1	White, no tanning
2	White, maybe pigmented nevi, some tanning
3	Pale, some visible tanning
4	Pale, good tanning
5	Normal, good tanning
Pigmentation of skin during life	
1	None
2	Some
3	Distinct
Hair color	
1	Completely white
2	Silvery white
3	White with yellowish touch
4	Whitish blonde
5	Pale blonde
6	Medium blonde
7	Dark blonde
8	Red, red-blonde
9	Medium brown
10	Dark brown, black
Pigment formation in hair during life	
1	Not at all
2	Some
3	Distinct
Degree of iris translucency	
1	Peripheral punctate iris translucency (only visible with confocal light, slit lamp)
2	Diffuse peripheral iris translucency, near pupillary border not translucent
3	Diffuse peripheral iris translucency, lens margin clearly visible through iris, pupillary margin not translucent
4	Complete iris translucency, including the pupillary margin
Degree of hypopigmentation of the retinal pigment epithelium and of foveal hypoplasia	
1	Peripheral retinal hypopigmentation, foveal structures visible
2	Peripheral distinct and centrally visible hypopigmentation, macular reflex visible, foveal reflex not visible
3	Pronounced peripheral and central hypopigmentation, foveal and macular hypoplasia
4	Grade 3 plus atypical choroidal vessels crossing the presumed macular region
Degree of morphologic anomaly of optic nerve head	
0	ONH not pathologic
1	ONH pale, normal size
2	ONH small, vital color
3	ONH small and pale
4	Dysplasia of ONH



FIGURE 2. Reformatted image along the optic nerves and tracts through the optic chiasm in a typical subject with albinism, showing a narrow chiasm and larger angles between optic nerves and tracts.

The differences in diameter of the optic nerves and tracts between the subjects with albinism and the normally pigmented control subjects are subtle and close to the resolution of the MRI sequence used. However the measured difference between the two groups are statistically significant. We therefore conclude that the optic nerves and tracts are smaller in humans with albinism, but that further imaging studies, using an even higher resolution, are advisable to quantify the differences exactly.

The second method we used to explore differences in the architecture of the optic chiasm between humans with albinism and normally pigmented subjects was based on a voxel-



FIGURE 3. Reformatted image along the optic nerves and tracts through the optic chiasm in a typical normally pigmented subject, showing a broad chiasm and small angles between optic nerves and tracts.

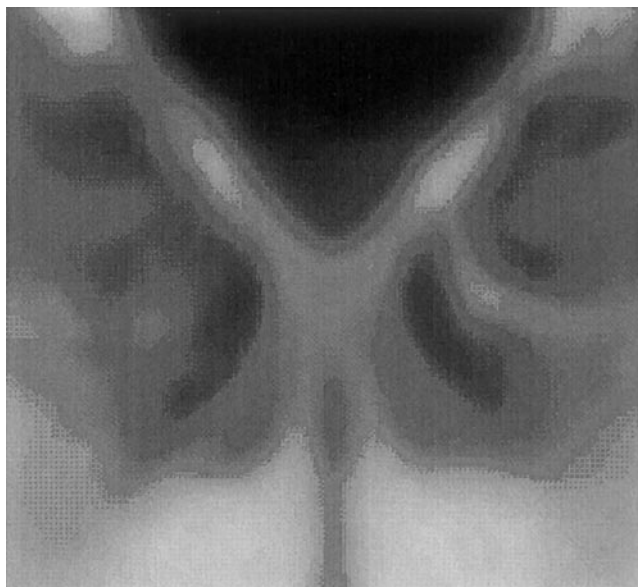


FIGURE 4. Mean image of the chiasmal region of subjects with albinism reformatted along optic nerves and tracts showing a small chiasm with large angles between optic nerves and tracts.

-by-voxel statistic. We did not use anatomic normalization before the voxel-by-voxel comparisons, because there is no accepted method for normalizing the chiasm region only. Therefore, additional intersubject variability is introduced that causes a lower sensitivity of the statistical tests and makes false-negative results more likely. However, our results remain on a high significance level with maximum T-scores up to 9.

In contrast to the method described herein, this voxel-based method is completely independent of any observer measurements, because it relies only on a *t*-test statistic on a voxel-by-voxel basis. Mean images were calculated as shown in Figures 4 and 5, in which the mean chiasm of subjects with albinism looked narrower than that of normally pigmented control subjects, and this difference was tested for significance by *t*-test.



FIGURE 5. Mean image of the normally pigmented control group, showing a rather wide chiasm with small angles between optic nerves and tracts

TABLE 3. Measured Distances and Angles

Group		A Diameter Right Optic Nerve	B Diameter Left Optic Nerve	C Chiasm Width	D Diameter Right Optic Tract	E Diameter Left Optic Tract	Chiasm Height	α Angle between Optic Nerves	β Angle between Optic Tracts
Albino	Mean	4.5	4.6	10.3	3.3	3.3	2.8	78	94
	SD	0.3	0.3	0.8	0.3	0.4	0.5	6	6
	Range	3.7-4.9	3.7-4.9	9.0-11.6	2.5-3.7	2.3-3.9	2.1-3.4	65-90	84-108
Control	Mean	5.2	4.9	12.9	3.7	3.7	2.5	69	79
	SD	0.5	0.4	0.8	0.5	0.4	0.3	5	8
	Range	4.1-6.0	4.1-5.5	11.3-14.0	3.1-5.0	3.2-4.9	1.8-3.0	62-76	67-96
Exact Significance (two-tailed)*		<0.01	<0.01	<0.001	<0.01	<0.01	<0.05	<0.01	<0.01

Measured distances and angles as labeled in Figure 1. All measurements described were significantly different. Measurements of distance are expressed in millimeters and of angles are expressed in degrees.

* By Mann-Whitney test.

The main disadvantage is that no quantitative measures were obtained. By using this kind of voxel-based statistics we were able to show that the differences in the architecture of the optic chiasm in humans with albinism are due to smaller lateral aspects of the chiasm. This is in line with the known fact that there are more crossed fibers in humans with albinism and that the uncrossed fibers in humans are confined to the lateral aspects of the optic chiasm. Optic nerves and tracts are on the same line in humans with albinism, which in turn leads to the larger angles between the optic nerves in this group.

A previous MRI study of the visual pathways in humans with albinism¹⁵ failed to show any abnormalities in size of the optic chiasm. There are several possible explanations for the results. The group of subjects with albinism was smaller (10 subjects with albinism versus 17 in our study), the study did not include a normally pigmented control group measured in the same

way, and the images were not reformatted in an axial oblique plane parallel to the optic nerves and tracts. In addition, the spatial resolution of the used MRI sequence was lower (1.2 mm vs. 1.0 mm voxel size) rendering the study less sensitive. We therefore conclude, that the methods in our study were more appropriate to show the difference in chiasm architecture between humans with albinism and normally pigmented subjects.

In summary, we have shown that the atypical crossing of optic fibers in humans with albinism changes the configuration of the optic chiasm as expected.

References

- Hubel DH, Wiesel TN. Receptive fields and functional architecture of monkey striate cortex. *J Physiol (Lond)*. 1968;195:215-243.
- Guillery RW, Okoro AN, Witkop CJ. Abnormal visual pathways in the brain of a human albino. *Brain Res*. 1975;96:373-377.
- Creel DJ, Witkop CJ, King RA. Asymmetric visual evoked potentials in human albinos: evidence for visual system anomalies. *Invest Ophthalmol*. 1974;13:430-440.
- Dräger UC. Birth dates of retinal ganglion cells giving rise to the crossed and uncrossed optic projections in the mouse. *Proc R Soc Lond B Biol Sci*. 1985;224:57-77.
- Ilia M, Jeffery G. Retinal mitosis is regulated by dopa, a melanin precursor that may influence the time at which cells exit the cell cycle: analysis of patterns of cell production in pigmented and albino retinae. *J Comp Neurol*. 1999;405:394-405.
- Jeffery G. Architecture of the optic chiasm and the mechanisms that sculpt its development. *Physiol Rev*. 2001;81:1393-1414.
- Baker, GE, Jeffery G. Distribution of uncrossed axons along the course of the optic nerve and chiasm of rodents. *J Comp Neurol*. 1989;289:455-461.
- Jeffery G. Distribution of uncrossed and crossed retinofugal axons in the cat optic nerve and their relationship to patterns of fasciculation. *Vis Neurosci*. 1990;5:99-104.
- Hoyt WF, Luis O. Visual fibre anatomy in the infrageniculate pathway of the primate. *Arch Ophthalmol*. 1962;68:64-106.
- Hoyt WF, Luis O. The primate optic chiasm: details of visual fibre organization studied by silver impregnation techniques. *Arch Ophthalmol*. 1963;70:69-85.
- Horton JC. Willebrand's knee of the primate optic chiasm is an artifact of monocular enucleation. *Trans Am Ophthalmol Soc*. 1997;95:579-609.
- Naito J. Retinogeniculate projection fibers in the monkey optic chiasm: a demonstration of the fiber arrangement by means of wheat germ agglutinin conjugated to horseradish peroxidase. *J Comp Neurol*. 1994;346:559-571.

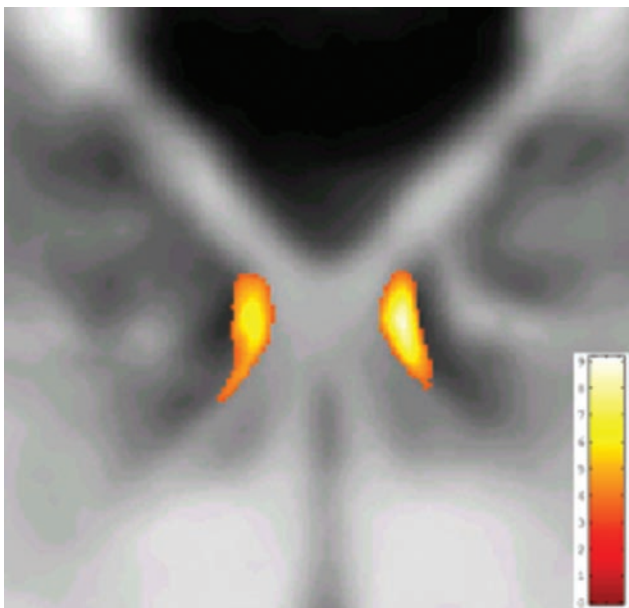


FIGURE 6. Statistical parametric (T) map of the chiasmal region. Overlay shows the mean albino image. Colored spots: voxels that show a significantly higher signal intensity in control subjects than in patients, which means that colored regions belong to the chiasm in control subjects but not in patients. Color reflects T scores as indicated in the color bar on the right side.

13. Brodsky MC, Glasie CM, Creel DJ. Magnetic resonance imaging of the visual pathways in human albinos. *J Pediatr Ophthalmol Strabismus*. 1993;30:382-385.
14. Käsmann-Kellner B, Ruprecht KW. Albinismus: Klassifikation und klinisches Spektrum. *Z Prakt Augenbeilkd*. 1999;20:189-203.
15. Passmore L, Käsmann-Kellner B, Weber BHF. Novel and recurrent mutations in the tyrosine gene and in the p gene in the German albino population. *Hum Genet*. 1999;195:200-210.
16. Mugler JP, Brookeman JR. Three-dimensional magnetization-prepared rapid gradient-echo imaging (3D MP RAGE). *Magn Reson Med*. 1990;15:152-157.
17. Ashburner J, Friston KJ. Voxel-based morphometry: the methods. *Neuroimage*. 2000;11:805-821.
18. Friston KJ, Holmes AP, Worsley KJ, Poline JB, Frith CD, Frackowiak RSJ. Statistical parametric maps in functional imaging: a general linear approach. *Hum Brain Map*. 1995;2:189-210.
19. Worsley KJ, Marrett S, Neelin P, Vandal AC, Friston KJ, Evans AC. A unified statistical approach for determining significant signals in images of cerebral activation. *Hum Brain Map*. 1996;4:58-73.
20. Wagner AL, Murtagh FR, Hazlett KS, Arrington JA. Measurement of the normal optic chiasm on coronal MR images. *AJNR Am J Neuroradiol*. 1997;18:723-726.
21. Parravano JG, Toledo A, Kucharczyk W. Dimensions of the optic nerves, chiasm and tracts: MR quantitative comparison between patients with optic atrophy and normals. *J Comput Assist Tomogr*. 1993;17:688-690.